Proceedings of the
Annual Stability Conference
Structural Stability Research Council
Louisville, Kentucky, April 1-4, 2025

Experimental study on the behavior of cold-formed steel lipped channels under uniform and non-uniform elevated temperatures

Jiangyue Xie[1], Thomas Gernay [2]

Abstract
This paper describes an experimental study on the behavior of load-bearing cold-formed steel (CFS) members under elevated temperatures from fire exposure. A custom-built electrical furnace with six independently controlled heating zones was installed in a loading frame, enabling testing of CFS members under uniform or non-uniform elevated temperatures. The ability to precisely control temperature gradients between the flanges allows testing a single member to failure under thermal conditions representative of a wall assembly exposed to fire on one side, capturing the effect of thermal gradient on the buckling behavior. Steady-state tests on short (18 in.) 600S200-54 lipped channels in compression were conducted at temperatures up to 600 °C, including tests with uniform temperatures and tests with 100°C gradient between the two flanges. Coupon tests were also conducted to characterize the material properties at elevated temperatures. The members lost about 23% of their strength at 400°C and 66% at 600 °C. For these short specimens under non-uniform heating, with one flange 100°C hotter than the other, the member strength fell between the strengths associated with the temperatures of the hot and cold flanges, with limited asymmetric effect on the local buckling response. This experimental data can support the development of design methods for CFS members in fire, enabling performance-based fire design.

1. Introduction

Cold-formed steel (CFS) is widely used in the U.S. for structural and non-structural components. In mid-rise buildings, CFS studs are notably used in load-bearing walls (Singh et al., 2022a). Extensive research on the behavior of lipped channel studs at ambient temperatures (Fratamico et al., 2018; Moen et al., 2008; Vieira et al., 2011) has lead to the development of design specifications (e.g., AISI S100-16). However, studies on the performance of CFS studs under fire conditions remain limited. Elevated temperatures from fire cause reductions in material properties such as elastic modulus and yield strength (Rokilan et al., 2020; Yan et al., 2021), affect the bracing from sheathing connections (Abreu et al. 2021), and generate thermal bowing and eccentricity effects when the heating is non-uniform (Vy et al., 2024). While some experiments have investigated the behavior of studs at elevated temperatures (e.g., Ranawaka et al., 2009; Gunalan et al., 2015), there remains a need for more test data including under non-uniform heating. Temperature gradients commonly develop in CFS studs when used in wall assemblies because the walls are subjected to fire on one side (Feng et al., 2005; Torres et al., 2023). Understanding the strength and buckling behavior of CFS members under such heating conditions is therefore crucial.

[1] Ph.D Candidate, Johns Hopkins University, <jxie47@jhu.edu>
[2] Assistant Professor, Johns Hopkins University, < tgernay@jhu.edu >

This paper describes a study on CFS lipped channels in compression under uniform and non-uniform elevated temperature conditions. The study is part of a multi-scale effort to characterize the fire performance of CFS structures (Fig. 1). Experiments on material and members are conducted at JHU. To conduct the member experiments, a custom test rig was designed and built. The test rig features a flexible electrical furnace with six independently controlled heating zones, where the heating is generated with electrical ceramic heating pads. Steady-state tests were conducted on the CFS studs at temperatures up to 600°C, either with or without a temperature gradient between the flanges. Additionally, material coupon tests were conducted to obtain elevated temperature properties. In parallel, a full-scale 10-story CFS building (‘CFS-10’) is currently under construction on the UC San Diego outdoor shake table (esec.ucsd.edu), as part of the CFS-NHERI project funded through the NSF (PIs Hutchinson and Schafer) (Singh et al., 2022b). The test data collected at JHU at the material and member scales are used in simulation models for the structural fire modeling tasks for planning and future analysis of the full-scale building experiment. The overall goal of this effort is to advance performance-based structural fire design methods for CFS-framed structures (Yan and Gernay, 2022).

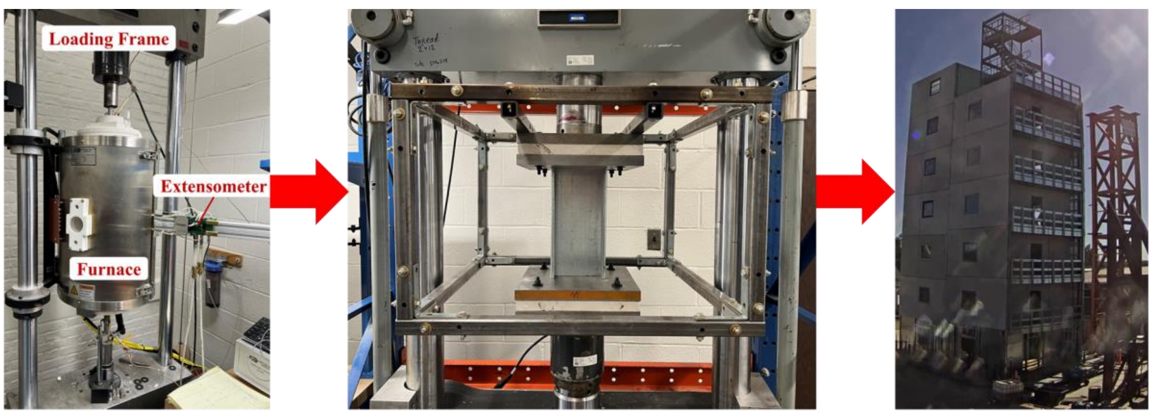

Test rig for the coupon tests　　Lipped channel installed in the test rig　　10-story building (cfs10.ucsd.edu)

Figure 1: Multiscale effort for structural fire testing of CFS structures: from coupon and member experiments (JHU) to full-scale CFS-framed building (CFS-10 at UCSD).

2. Specimens

The specimens used in this study are cold-formed steel (CFS) lipped channels measuring 475.2 mm (18 in.) in length, with 600S200-54 cross-section. The 600S200-54 members, generously donated by Unarco, are unpainted, uncoated, and unpunched, with a nominal yield strength of 345 MPa (50 ksi). The selection of the cross-section was aimed to isolate local buckling in the experiments of the short specimens. The specimens were tested under bare-bare boundary conditions with direct contact between the studs and the loading plates.

2.1 Specimen dimensions

The nominal dimensions of the cross-section is provided in Table 1 and illustrated in Fig. 2. The effective cross-sectional area is 214 mm². The calculated nominal yield axial capacity (P_y) is 73.9 kN for the 600S200-54 studs.

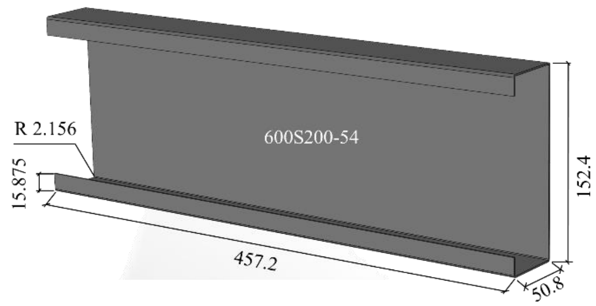

Figure 2: Dimensions of the 600S200-54 lipped channel specimen (unit: mm).

Table 1. Nominal dimensions of the 600S200-54 cross-section

Specimen	Unit	Web depth	Flange width	Stiffening lip	Thickness	Fillet radius
600S200-54	mm.	152.4	50.8	15.875	1.438	2.156
	in.	6	2	0.625	0.0566	0.0849

2.2 Material properties

To evaluate the strength and retention factors of the materials, coupon specimens were prepared from the studs in accordance with ASTM E21 (2009) and ASTM E8 (2016). These specimens were designed for pin-loaded tensile tests conducted at both ambient and elevated temperatures. The coupons have a gauge length of 50.8 mm (2 in.) and a width of 12.7 mm (0.5 in.), see Fig. 3. The coupon tests were performed under steady-state conditions, with a controlled heating rate of 10 °C/min and a loading rate of 0.25 mm/min, according to the procedure described in Yan et al. (2020). Tests were conducted at five temperatures: 20 °C, 300 °C, 400 °C, 500 °C, and 600 °C. The resulting elastic modulus, ultimate strength, and yield strengths (at 0.2% and 2% plastic strain) of the material at ambient temperatures are given in Table 2. Additionally, the retention factors of the mechanical properties at elevated temperatures are provided in Table 3. These retention factors are required for the analyses under fire conditions.

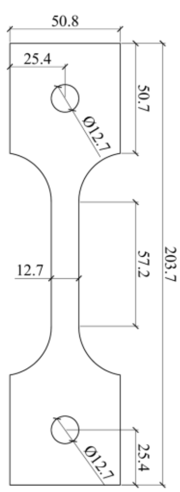

(a) Dimensions (unit: mm)

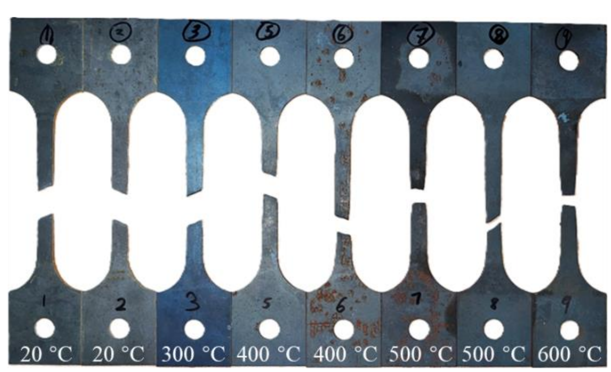

(b) Coupon from 600S200-54 studs

Figure 3: Coupon specimens

Table 2: Material properties at ambient temperature

Specimen	Elastic modulus (MPa)	Ultimate strength (MPa)	$f_{y,0.2}$* (MPa)	$f_{y,2}$** (MPa)
600S200-54	205,511	462	407	405

*$f_{y,0.2}$ is the yield strength at 0.2% plastic strain
**$f_{y,2}$ is the yield strength at 2% strain

Table 3. Retention factors for the cold-formed steel from the 600S200-54 studs at elevated temperatures

T (°C)	k_E	$k_{y,0.2}$	$k_{y,2}$	k_u
20	1.000	1.000	1.000	1.000
300	0.855	0.801	0.946	0.942
400	0.543	0.660	0.756	0.726
500	0.486	0.480	0.544	0.496
600	0.201	0.302	0.296	0.275

3. Experimental setup

The experiments on the short CFS lipped channels were conducted under combined compressive loading and elevated temperatures. The specimens were first heated within a custom-designed furnace, then loaded to failure (steady-state tests). The furnace system comprised an external frame supporting an insulation blanket and six independently controlled electric heating pads, as shown in Fig. 4. Throughout the experiments, data including load, displacement, and the temperature at the surface of the steel stud in each heating zone were continuously monitored and recorded using LabVIEW software on a connected computer.

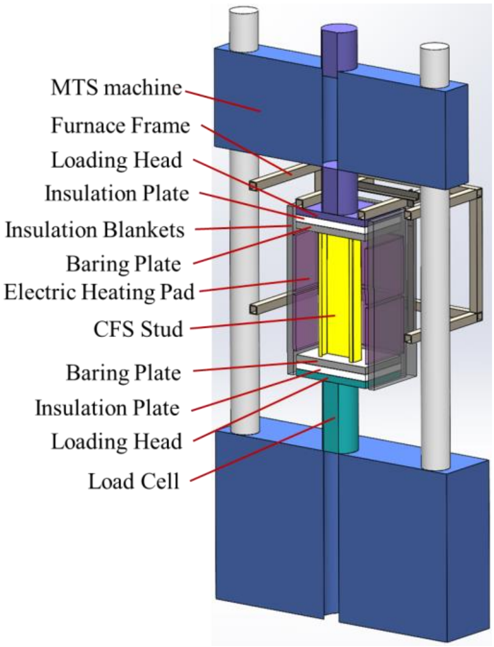

(a) 3D cut view

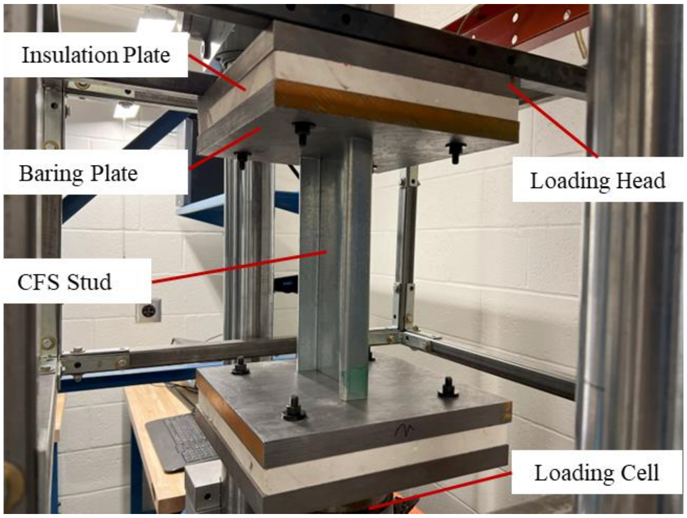

(b) Inside the furnace

Figure 4: Test setup for elevated temperature testing of CFS members in the MTS machine.

3.1 Elevated temperature testing rig

To heat the specimens, a custom furnace was designed and built, to be installed in the MTS loading area. The custom furnace includes a frame, constructed from steel box members, with angle steel kits to suspend insulation blankets and electric heating pads. The insulation blankets serve to minimize heat loss. Inside the blankets, eight electric heating pads are used to heat the steel specimen. The heating pads are controlled using six independent controllers, connected to thermocouples measuring temperatures on the surface of the specimen (web and flanges). This allows controlling the heating rate and the temperature distribution on the member. The furnace setup allows for the specimens to be heated uniformly or with controlled non-uniform temperatures gradients. Hard insulation plates were attached to the loading heads to reduce heat transfer and protect both the MTS machine and its load cell from thermal damage. Additionally, bearing plates were incorporated to enhance the stiffness of the contact surfaces and prevent the insulation plates from being crushed under load. This setup ensured consistent thermal and mechanical conditions for an accurate evaluation of the structural response of the CFS studs under elevated temperatures.

3.2 MTS Loading system

The loading system is an MTS universal testing machine, with a maximum capacity of 45 tons (100 kips). During the first phase of the test, the specimen is heated to the target temperature, and a force-control method is used to maintain a constant (low) initial load on the studs, with constant adjustment of the position of the loading heads to compensate for thermal expansion. The initial applied load, ranging from 0.6 kN to 1.2 kN, served to maintain the stud in position on its two end plates. Once the target temperatures were achieved, a stabilization period was allowed. Then, in the second phase of the test, the specimen is loaded under a displacement-control method. A controlled loading rate of 0.0635 mm/min was used up to failure of the specimen, defined as a post-peak reduction of the applied load to 75% of the peak load value. The load and displacement data were captured by the MTS system and load cell connected to the computer for control and data acquisition.

3.3 Electrical heating system

Electrical ceramic heating pads were secured to angle steel parts using screws. To independently heat the upper and lower flanges and web of the stud specimens, eight heating pads were installed within the furnace, powered by a dedicated heating control system. The furnace was divided into six heating zones: three zones in the upper section and three in the lower section (see Fig. 5a). In the upper section, two heating pads were independently controlled to heat the left and right flanges, while the remaining two pads simultaneously heated the upper web. The lower section followed the same configuration, with independent control of heating pads for the lower flanges and web. The temperature control system operated based on real-time feedback from thermocouples placed within the furnace (see Fig. 5b). The control machine featured six independent outputs, each corresponding to one of the six heating zones. This design allowed precise regulation of heating parameters, including heating rates, target temperatures, and soaking durations, providing the flexibility to simulate a variety of thermal conditions for steady-state tests.

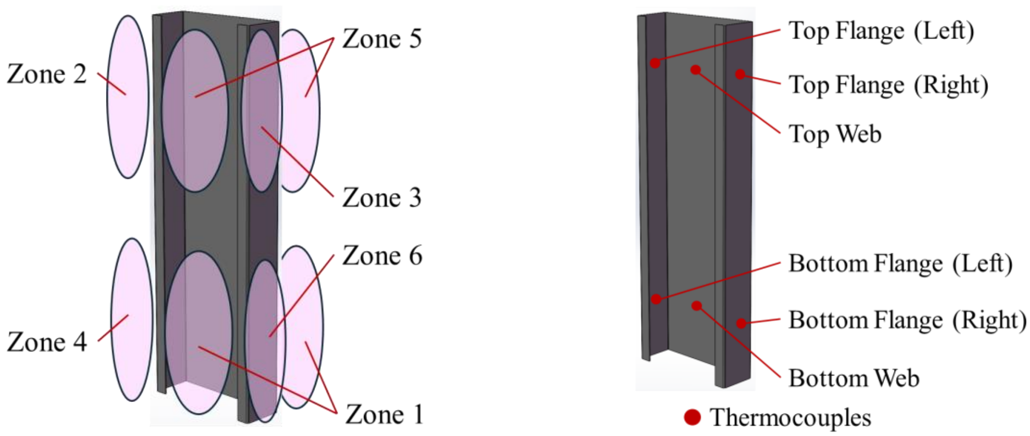

(a) Six heating zones (b) Thermocouple layouts

Figure 5: Setup for electrical heating of the CFS members installed in the rig.

3.4 Temperature Distribution

The stud specimens were heated to specified target temperatures and allowed to stabilize before being loaded to failure in steady-state tests. The maximum temperature applied to the studs in this study was 600°C in both uniform and non-uniform conditions. For uniform heating, the six zones of the furnace were heated to the same target temperature, to obtain a uniform temperature distribution across the specimen. In contrast, non-uniform heating involved creating and maintaining a temperature gradient of 100°C between the two flanges of the stud. For example, one flange of the stud was heated to 600°C while the other flange was heated to 500°C. The temperature distributions for both types of heating conditions are illustrated in Fig. 6.

Fig. 7 plots the measured temperatures during the tests under uniform elevated temperatures. The plot includes the temperatures measured at each specific point, along with the average temperature for each test. Fig. 8 plots the measured temperatures for the studs subjected to non-uniform heating conditions. The plots include the average temperatures of the hot and cool flanges, demonstrating the stability of the temperature gradients. Once thermal equilibrium was achieved, the required temperatures for both flanges in each test were maintained, ensuring a consistent 100°C gradient between the hot and cool flanges. These results confirm the precise temperature control achieved during the experiments, and the ability of the custom heating system to generate controlled temperature profiles for testing of the CFS members.

3.5 Test Matrix

The test matrix is shown in Table 4. Each test was repeated twice. For uniform heating, the specimens were tested at temperatures of 20°C, 300°C, 400°C, 500°C, and 600°C. For non-uniform heating, temperature gradients were applied between the flanges, with the cooler flange at 300°C and the hotter flange at 400°C, the cooler flange at 400°C and the hotter flange at 500°C, as well as the cooler flange at 500°C and the hotter flange at 600°C, respectively.

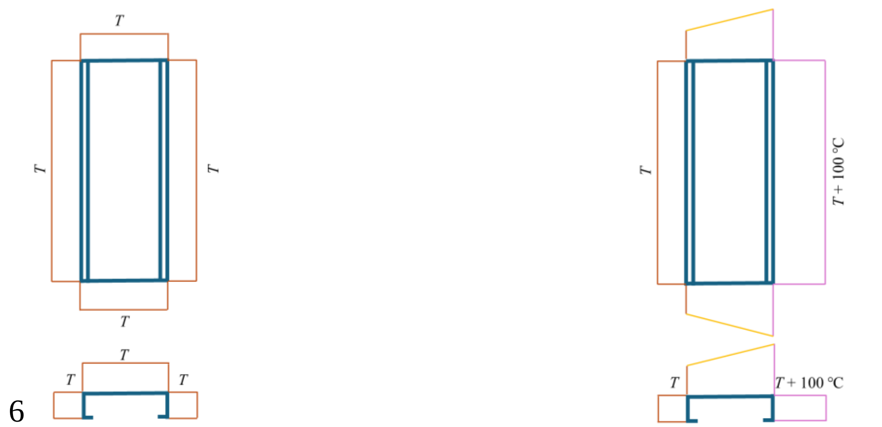

(a) Uniform heating (b) Non-uniform heating

Figure 6: Temperature distribution applied to the CFS studs.

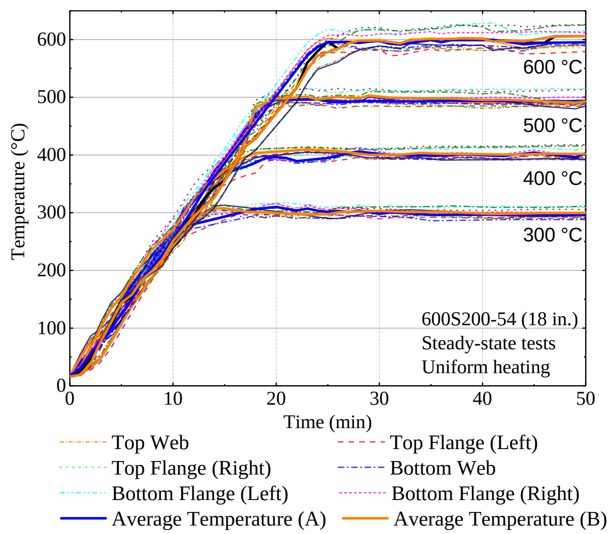

Figure 7: Temperature measurements during uniform steady-state tests on lipped channel studs.

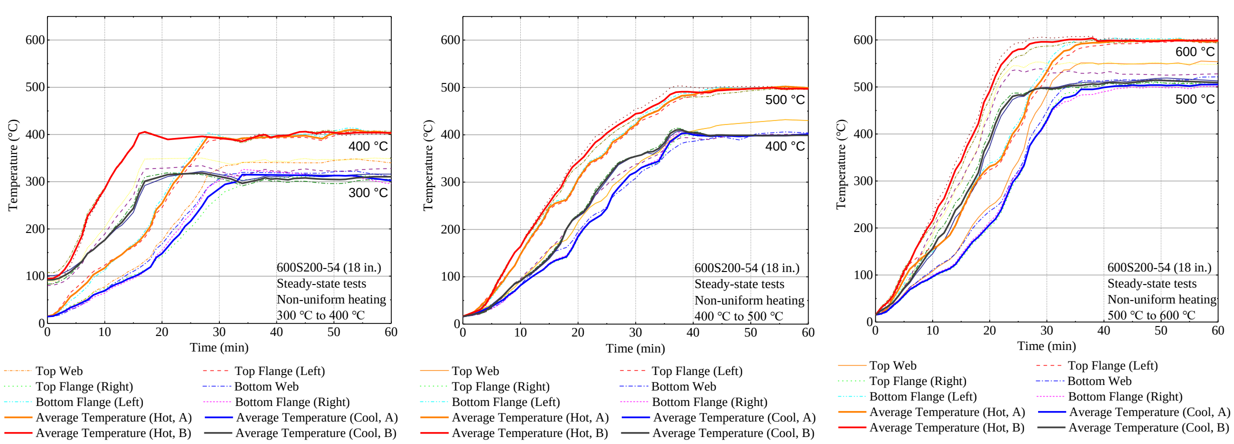

(a) 300°C to 400°C (b) 400°C to 500°C (c) 500°C to 600°C

Figure 8: Temperature measurements during non-uniform steady-state tests on lipped channel studs.

Table 4: Test matrix

Test Protocol	Specimen	Length	Thermal Control	Number
Steady-state test Loading to failure	600S200-54	457.2 mm (18 in.)	Ambient temperature	2
			Uniform 300 ℃	2
			Uniform 400 ℃	2
			Uniform 500 ℃	2
			Uniform 600 ℃	2
			Non-uniform 300 ℃ to 400 ℃	2
			Non-uniform 400 ℃ to 500 ℃	2
			Non-uniform 500 ℃ to 600 ℃	2

4. Results from the tests on the lipped channel columns

This Section discusses the experimental results from the experiments listed in Table 4. The experiments were conducted in the Multi-Hazard Resilient Structures laboratory at Johns Hopkins University in the summer and fall of 2024.

4.1 Strength and displacements

At ambient temperature, the mean peak load (i.e., measured member strength) of the 600S200-54 studs was 101.02 kN. At elevated temperatures, the member strength and corresponding member retention factors are given in Table 5. The results indicate that the strength decreases significantly with increasing temperatures. At 600°C, the strength of the 600S200-54 stud is reduced from 101.02 kN to 34.19 kN, corresponding to 34% of the ambient temperature value.

The member retention factors are plotted in Fig. 9. These factors are obtained by dividing the measured elevated temperature member strength by the ambient temperature strength. Interestingly, for non-uniformly heated specimens, the member strength falls between the corresponding strengths for specimens heated uniformly at the level of either the hotter or cooler flange. This suggests that, for the tested short specimens, there is a limited effect of the thermal gradient on the strength. Additionally, it seems conservative to evaluate the member strength based only on the hot flange temperature, as is sometimes recommended in design methods. These observations are based on experiments on short specimens of one given section type exhibiting local buckling, and different effects could come into play when testing different sections, or longer specimens which are more sensitive to thermally-induced differential deformations.

The load-displacement curves of the tested studs are plotted in Fig. 10. The progressive reduction of member stiffness and strength with temperature is visible. The experiments also show a good repeatability. For the studs subjected to non-uniform heating, the differential thermal expansion and reduction of properties results in non-uniform strains and stresses in the member. Buckling may initiate in the hotter part of the section as it is weaker, resulting in a redistribution of stresses toward the cooler part. This results in more complex member stiffness variation patterns in Fig. 10 compared with the uniform heating tests. These observations underline the influence of temperature distribution on the mechanical response of CFS studs, particularly under non-uniform heating conditions, where load transfer mechanisms and buckling behaviors may differ from those under uniform heating.

Table 5: Test Results

Num.	Temperature	600S200-54	
		Peak Load (kN)	Retention Factor
1	20 °C	103.11	1.000
2		98.93	
3	Uniform 300 °C	87.32	0.86
4		90.39	0.89
5	Non-uniform 300 °C - 400 °C	89.10	0.88
6		86.30	0.85
7	Uniform 400 °C	77.75	0.77
8		78.11	0.77
9	Non-uniform 400 °C - 500 °C	67.26	0.67
10		66.63	0.66
11	Uniform 500 °C	57.69	0.57
12		-	-
13	Non-uniform 500 °C - 600 °C	39.06	0.39
14		41.99	0.42
15	Uniform 600 °C	33.27	0.33
16		35.10	0.35

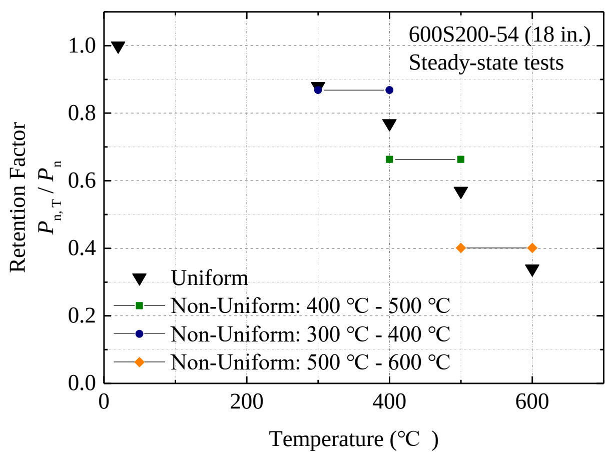

Figure 9. Retention factors of 600S200-54 lipped channels in compression in steady-state tests.

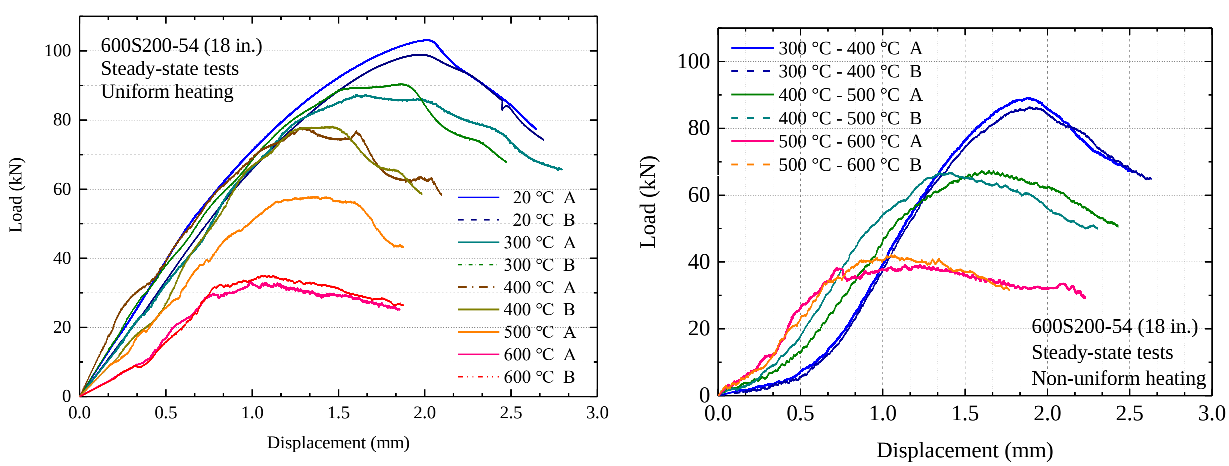

(a) Steady-state tests with uniform heating

(b) Steady-state tests with non-uniform heating

Figure 10: Steady-state tests on 600S200-54 lipped channels in compression.

4.2 Failure modes

Pictures of the specimens after the tests are shown in Fig. 11 (uniform temperature tests) and Fig. 12 (non-uniform temperature tests). For the tested 600S200-54 studs, local buckling of the web was clearly observed in the experiments, under both uniform and non-uniform temperature distributions. Inwards or outwards displacement of the flanges indicative of distortional buckling is observed to various degrees in several specimens. Local buckling also appeared on the lips and flanges in some cases, notably at temperatures of 400 °C and above. Furthermore, under non-uniform heating with 100 °C gradient, a slightly larger buckling deformation could be observed on the hot flange compared with the cool flange, but the effect was limited. It is also noteworthy that several researchers noted the effect of initial geometric imperfections on the buckling mode (Feng et al., 2003), which could explain variations in final deformed shapes between replicate tests.

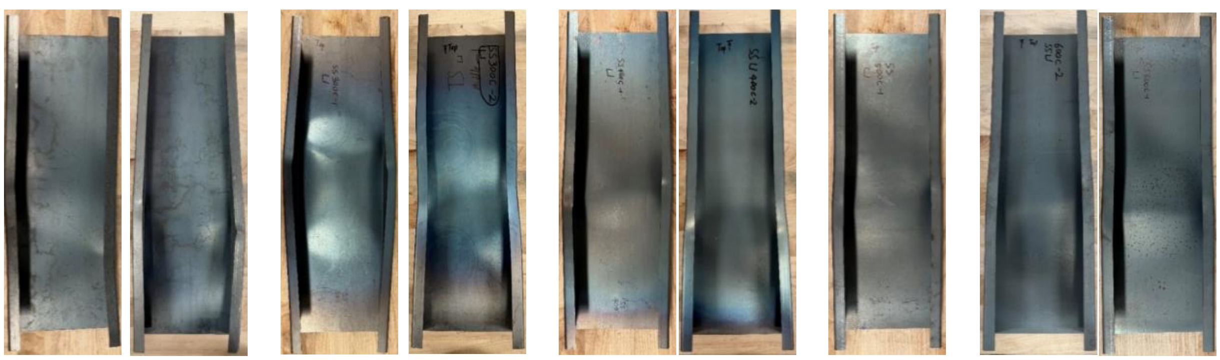

(a) 20 °C (b) 300 °C (c) 400 °C (d) 500 °C (d) 600 °C

Figure 11: 600S200-54 lipped channel specimens at failure, tests with uniform heating.

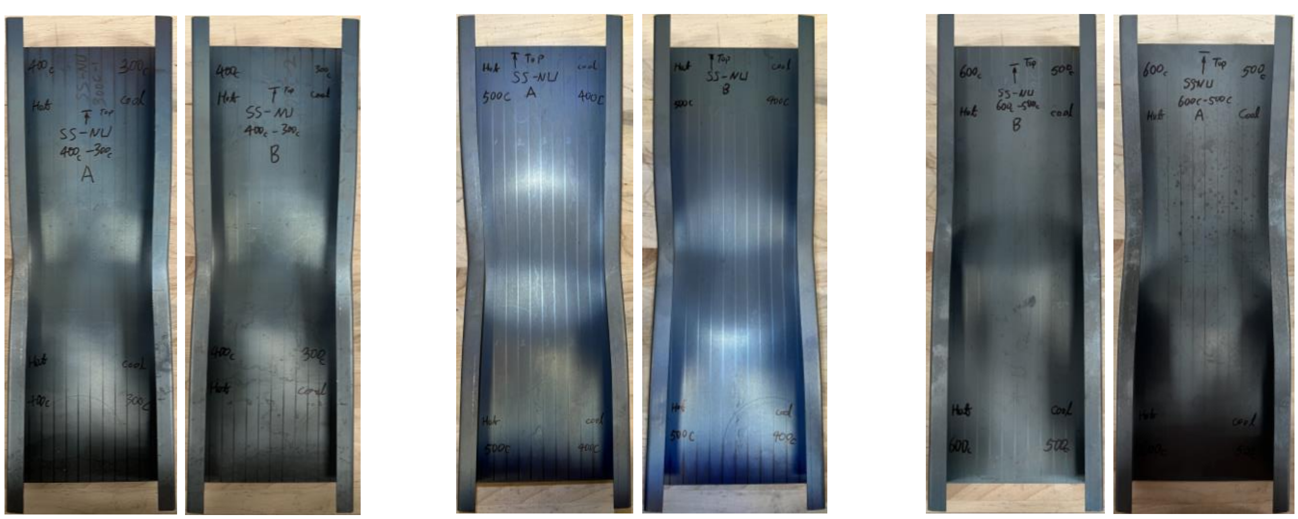

(a) 300 °C- 400 °C (b) 400 °C- 500 °C (b) 500 °C- 600 °C

Figure 12: 600S200-54 lipped channel specimens at failure, tests with non-uniform heating.

5. Conclusions

This study investigated the behavior of cold-formed steel lipped channels under the combined effect of compressive loading and elevated temperatures. A major objective was the development of an experimental setup to enable precise temperature control to test CFS members under both uniform and non-uniform temperature conditions. The custom-built electrical furnace was shown to achieve accurate and repeatable heating of the CFS specimens up to 600°C, including with controlled gradient of 100°C between the flanges. This experimental setup can be used to characterize the strength and buckling behavior of load bearing CFS members under fire conditions. The application of non-uniform heating, in particular, allows reproducing the thermal exposure seen in wall or floor assemblies, but on a single member with controlled mechanical and thermal boundary conditions.

Experiments conducted on short studs with 600S200-54 cross-section showed significant reduction in stiffness and ultimate strength with temperature increase. Under uniform temperature, the members retained about 77% of their strength at 400°C and 34% at 600 °C. Local buckling was observed on the web, and to some extent on the flanges and lip for specimens at temperatures of 400°C and above. Distortional buckling was also observed. Non-uniform heating introduced asymmetry in the material properties and thermal expansion. Yet, in the tested short specimens, the 100°C temperature gradient did not significantly change the buckling behavior. In terms of strength, the studs tested under non-uniform temperature exhibited values between those of the member at the hot flange temperature and the member at the cold flange temperature.

Future studies will conduct experiments on longer members, different cross-sections, and with higher gradients, to continue investigating the effects of non-uniform heating on the stability and strength of CFS members in compression. It is expected that members subjected to distortional and/or global buckling may be more susceptible to thermal gradients. In the end, the data collected from these member experiments will be used to calibrate numerical models and advance methods for the fire design of CFS structures.

Acknowledgments

This research was supported by the National Science Foundation (NSF) through award #2237623 "CAREER: Performance-Based Fire Design for Cold-Formed Steel Structures" (PI T. Gernay, Program Manager J. Pauschke, CMMI). The financial support is gratefully acknowledged.

We are thankful to Unarco Material Handling, Inc. and to Jim Crews for the donation and transport of the lipped channels. We also thank Senior Technician Nickolay Logvinovsky for his assistance in the laboratory, JHU Master student Joshua Dillard for his help with coupon testing, and Prof. Ben Schafer for his invaluable advice in developing the experimental program and test setup.

References

Abreu J.C., Vieira Jr L., Gernay T., Schafer B.W. (2021). "Cold-formed steel sheathing connections at elevated temperature". *Fire Safety Journal*, 123, 103358

AISI-S100-16, North American Specification. (2016). "For The Design of Cold-formed Steel Structural Members, American Iron and Steel Institute. Washington DC, USA.

ASTM. (2009). "ASTM E21, Standard Test Methods for Elevated Temperature Tension Tests of Metallic Materials." *American Society for Testing and Materials,* West Conshohocken, PA.

ASTM. (2016). "ASTM E8/ E8M-16, Standard Test Methods for Tension Testing of Metallic Materials." *American Society for Testing and Materials*, West Conshohocken, PA.

Feng M., Wang Y.C., Davies J.M. (2003). "Structural behaviour of cold-formed thin-walled short steel channel columns at elevated temperatures. Part 1: experiments", *Thin-Walled Structures* 41 543–570.

Feng M., Wang Y.-C. (2005). "An experimental study of loaded full-scale cold-formed thin-walled steel structural panels under fire conditions", *Fire Safety Journal* 40 43–63.

Fratamico D.C., Torabian S., Zhao X., Rasmussen K.J.R., Schafer B.W. (2018). "Experimental study on the composite action in sheathed and bare built-up cold-formed steel columns." *Thin-Walled Structures* 127, 290–305.

Gunalan S., Heva Y.B., Mahendran M. (2015). "Local buckling studies of cold-formed steel compression members at elevated temperatures." *Journal of Constructional Steel Research*. 108 31-45.

Moen C.D., Schafer B.W.. (2008). "Experiments on cold-formed steel columns with holes." *Thin-Walled Structures*, 46, 1164-1182.

Ranawaka T., Mahendran M. (2009) "Distortional buckling tests of cold-formed steel compression members at elevated temperatures." *Journal of Constructional Steel Research*. 65 249-259.

Rokilan M., Mahendran M. (2020). "Elevated temperature mechanical properties of cold-rolled steel sheets and cold-formed steel sections." *Journal of Constructional Steel Research.* 167 105851.

Singh A., Hutchinson T., Torabian S., Schafer B., Peterman K., Padgett L., Jones H. (2022a). "Structural design narrative of the CFS-NHERI 10-story test building for multi-dimensional shake table testing." *Cold-Formed Steel Research Consortium (CFSRC) Colloquium*.

Singh A., Wang X., Zhang Z., Derveni F., Castaneda H., Peterman K. D., Schafer B.W., Hutchinson T.C. (2022b). Steel Sheet Sheathed Cold-Formed Steel Framed In-line Wall Systems. I: Impact of Structural Detailing. *Journal of Structural Engineering*, 148(12), 04022193

Torres L., Couto C., Real P.V., Piloto P. (2023). "Numerical study of the fire behaviour of external walls in light steel framing". *Fire Safety Journal*, 141, 103946.

Vieira Jr L., Shifferaw Y., Schafer B.W. (2011). "Experiments on sheathed cold-formed steel studs in compression." *Journal of Constructional Steel Research*. 67 1554-1566.

Vy S. T., Ariyanayagam A., Mahendran M. (2024). "Behaviour and design of CFS stud walls under both sides fire exposure". *Thin-Walled Structures*, 197, 111619.

Yan X., Xia Y., Blum HB., Gernay T. (2020). "Elevated temperature material properties of advanced high strength steel alloys". *Journal of Constructional Steel Research*, 174, 106299

Yan X., Abreu J.C.B., Glauz R.S., Schafer B.W., Gernay T. (2021) "Simple Three-Coefficient Equation for Temperature-Dependent Mechanical Properties of Cold-Formed Steels." *Journal of Structural Engineering*. 147 (4) 04021035.

Yan X., Gernay T. (2022). "Structural fire design of load-bearing cold-formed steel assemblies from a prototype metal building". *Structures*, 41, 1266–1277